International Journal of Fluid Machinery and Systems
Vol. 1, No. 1, October-December 2008

Original Paper

Flow Analysis in Positive Displacement Micro-Hydro Turbine and Development of Low Pulsation Turbine

Junichi Kurokawa[1], Jun Matsui[1] and Young-Do Choi[2]

[1] Faculty of Engineering, Yokohama National University
79-5 Tokiwadai, Hodogaya-ku, Yokohama, 240-8501, Japan
[2]Industry-Academic Cooperation Foundation, Korea Maritime University
1 Dongsam-dong, Youngdo-ku, Busan, 606-791, Korea

Abstract

In order to extract micro hydropower in the very low specific speed range, a Positive Displacement Turbine (PDT) was proposed and steady performance was determined experimentally. However, the suppression of large pressure pulsation is inevitable for practical application of PDT. The objective of the present study is to reveal the mechanism and the characteristics of pressure pulsation in PDT by use of CFD and to suppress the pressure pulsation. Unsteady CFD analysis has revealed that large pressure pulsation is caused by large variation of rotational speed of the following rotor, while the driving rotor, which is output rotor, keeps constant speed. Here is newly proposed a 4-lobe helical type rotor which can reduce the pressure pulsation drastically and the performance prediction of new PDT is determined.

Keywords: Micro hydropower, Positive displacement turbine, Helical rotor, Pressure pulsation, Performance improvement

1. Introduction

Micro hydropower is one of the most cost-effective and reliable energy resources to be considered for providing clean electricity generation [1-5]. Particularly, in order to use the micro hydropower resources (below 100kW) effectively in the sites of very high head but relatively low flow rate, Phommachanh et al. [6] have proposed a positive displacement turbine (PDT), and the methods of a performance estimation and an optimum design of the turbine have been determined on the basis of experimental results for the turbine performance. Moreover, it has been clarified that a key problem for practical application of the PDT is the reduction of pressure pulsation and leakage in the turbine.

For the reduction of the pressure pulsation, a small sized simple surge tank installed at the inlet and outlet of the turbine was able to reduce the pulsation amplitude by 75%. However, it is necessary to make clear the mechanism of the pulsation in order to further reduce the pulsation without installing supplemental structures. Moreover, for the reduction of leakage, about 12% of efficiency improvement was attained by narrowing the side clearance from 60μm to 10μm, but it is necessary to examine the details of the internal flow for further improvement of the turbine efficiency.

The PDT is in principle similar to a positive displacement flow meter, a water pressure motor [7] and a hydraulic motor, but the internal flow characteristics are not almost clarified because of the difficulty in measurement. As there exists strong unsteadiness in the internal flow with a periodical fluctuation, CFD analysis for the flow field needs unsteady numerical simulation. However, because the unsteady analysis of the internal flow, which is caused by non-axisymmetric structure of a rotor and a casing, has some difficult problems such as the data transfer between the regions of a rotor and a stator, as well as the analysis of a very small gap, CFD analysis seems not to be completely performed yet according to author's review of related reference literatures.

This study is aimed to make clear the characteristics of the pressure pulsation and the leakage in a 3-lobe rotor type PDT by CFD analysis and experiment. Moreover, a new 4-lobe helical rotor type PDT is proposed to reduce pressure pulsation drastically and a performance estimation method and a design method for the new turbine are also proposed.

2. Experimental and Numerical Methods

2.1 Experimental Apparatus

Figure 1 shows experimental apparatus adopted in the present study. The clean water is supplied from a water tank ① to PDT by a multistage centrifugal pump ②. A filter ③ and a flow meter ④ are installed on the way. The effective head H can be varied

Received July 28 2008; revised September 3 2008; accepted for publication September 8 2008: Review conducted by Dr. Hideaki Tamaki.
Corresponding author: Young-Do Choi, Dr., ydchoi@pivlab.net

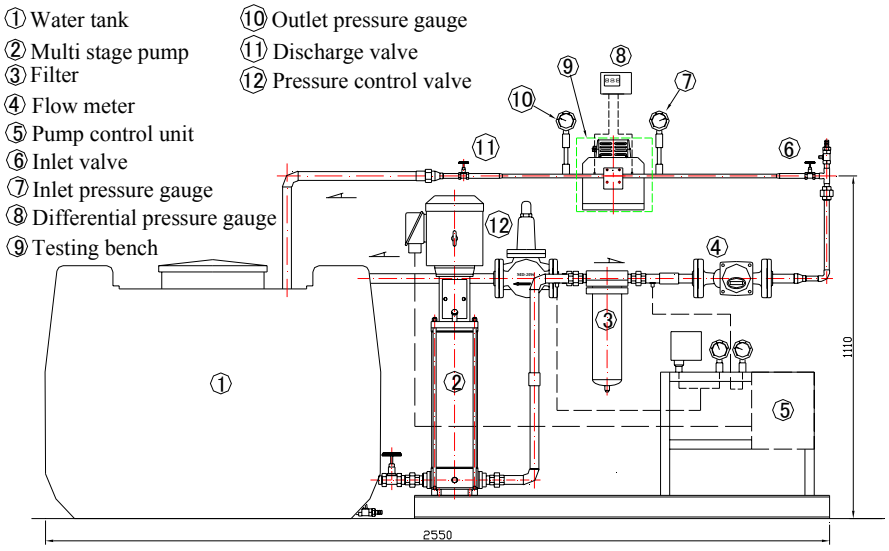

Fig. 1 Schematic view of testing system

by adjusting the rotational speed of the pump and adjusting the pressure control valve ⑫, and the flow rate Q is regulated by a control valve ⑥. A valve ⑪ is used for adjustment of the discharge pressure. Torque T acting on the rotors is measured by a torque meter and a mechanical load connected to the turbine axis.

Measurement of output axis torque is conducted by letting the load increase with a fixed flow rate. As the load increases, rotational speed reduces and then, flow rate decreases accordingly. Therefore, measurement is carried out by increasing effective head $H(=\Delta p/\rho g)$ with a fixed flow rate. Experiment is conducted in the range of flow rate Q=0-80l/min, head H=0-70m and rotational speed n=0-2800min^{-1}.

Figure 2 and Table 1 show the details of the micro PDT and its dimensions. The two PDT models are remodeled from commercial lobe-type flow meters, and consist of a twin rotor, 2 shafts, 4 bearings, a gasket, a casing and a casing cover. Details of the turbine in Fig. 2(a) are already reported in the previous study [6]. The turbine runner consists of a pair of 3-lobe type rotor, which is made of plastic resin with a diameter D=21.2mm, a height B=16.4mm, and 33 pieces of tooth are installed around the lobe to secure gearing of the 2 rotors each other. Figure 2(b) shows a newly developed micro PDT in this study, and the rotor has a diameter D=38.8mm and a height B=54.0mm. A pair of 4-lobe type rotor twists helically with a twist angle of γ=11deg., and therefore, it is expected that pressure pulsation in the turbine can be remarkably reduced because the contact point of 2 rotors moves linearly to the axial direction every moment.

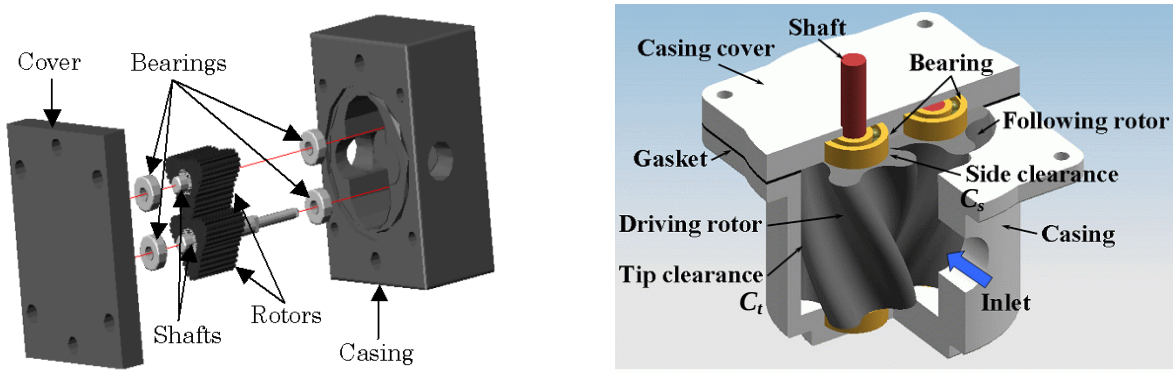

(a) 3-lobe straight type (b) 4-lobe helical type

Fig. 2 Positive displacement turbine design

Table 1 Dimensions of 3-lobe straight type and 4-lobe helical type

Descriptions	Unit	3-Lobe Turbine		4-Lobe Turbine
Rotor diameter (D)	mm	21.2		38.8
Height of rotor (B)	mm	16.4		54
Side-clearance (c_s)	μ m	60	10	100
Tip-clearance (c_t)	μ m	60	10	120
Twisted angle(γ)	deg.	0	0	11

If there is no leakage in the positive displacement type fluid machinery, theoretical flow rate Q_{th} is given by $Q_{th}=V_d n/60$, where V_d is volumetric displacement per 1 rotor revolution and n is rotational speed, but in actual case leakage flow rate Q_l occupies a large proportion of the total flow rate Q. Volumetric displacements for both PDT are $V_d=4.72\times10^{-6}$ m^3/rev for 3-lobe rotor, and $V_d=50.0\times10^{-6}$ m^3/rev for 4-lobe rotor, about 10 times larger than the former, respectively.

2.2 Numerical Analysis and Simulation Model

For the numerical analysis of the performance and internal flow characteristics of the 3-lobe PDT in Fig. 2(a), a commercial CFD code of ANSYS-CFX [8] is adopted. Fine hexahedral numerical grids are employed for the turbine passages to ensure relatively high accuracy of calculated results as shown in Fig. 3. The grid number of about 5.0×10^4 has been used for the numerical turbine model. Same length of the inlet and outlet pipes is determined to 20D. As a simulation model, turbine with smooth rotor circumferential boundary (gearless) is mainly used as shown in Fig. 3(a). In addition, the influence of rotor gear is examined using 2 kinds of rotor mesh, without gear and with gear around the rotor as shown in Figs. 3(a) and 3(b). Though the rotor has 3-dimensional shape with a side clearance between rotor side tip and casing wall, 2-dimesional numerical grid is used mainly in order to shorten the time of unsteady calculations. Three-dimensional numerical grid is also adopted as well to reveal the influence of side clearance. Actually the torque transmission is performed by the two rotors which come in contact with each other, but there is a gap between the two rotors in the numerical grid of the calculation model.

As a turbulence model, *SST* model is used, and averaged uniform flow at the inlet and a constant pressure at the outlet are adopted for the boundary conditions. In the case of 3-lobe rotor, which has a period of revolution angle of 60°, the unsteady calculation is almost converged after 2 periods of revolution when the results of a quasi-steady state calculation using a frozen rotor method [8] are used as the initial input condition for the calculation.

When a pair of rotor is contacted and rotated smoothly in a positive displacement rotary machine in a non-axisymmetric casing with a remarkably narrow tip clearance, the unsteady CFD analysis is necessary to perform the calculation of flow characteristics. As a method of numerical mesh generation, functions of mesh morphing and remesh are adopted in this study [8]. The shape of mesh can be transformed automatically with a rotor rotation from the initial state by the mesh morphing function as shown in Fig. 3(c), and then the mesh is reformed to the initial state when the transformation becomes large by the remesh function. The calculation restarts at a next adjacent rotor position by each rotation angle of 2° .

The dimensions of the model turbine for CFD analysis are determined to height of rotor B=2.0mm, tip clearance c_t=0.1mm or 0.05mm, center clearance between two rotors c_c =0.05mm. 11 layers of mesh are applied to tip and center clearances. Though circular pipes are installed at the rotor entrance and exit in experiment, the calculation model has adopted a 2-dimensional parallel duct as the shape of entrance and exit pipes hardly give influence on the pulsation. Moreover, as the Reynolds number based on the equivalent diameter of tip clearance is more than $Re=3\times10^3$, all flow fields including narrow clearance are treated as turbulent flow.

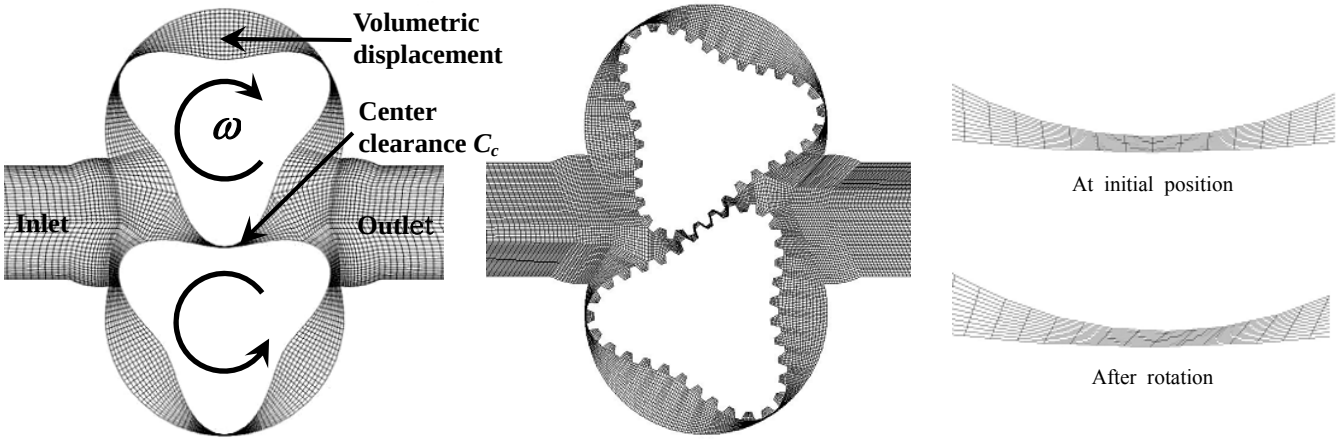

(a) Rotors with gearless lobe (b) Rotors with geared lobe (c) Automatic grid transformation

Fig. 3 Calculation model for CFD

Generally, when a pair of non-circular rotor rotates by coming in contact smoothly with each other, tangential velocities of both rotors at the contact point become equal. Therefore, the revolution speed of two 3-lobe rotors can not be constant, and thus the revolution speed varies every moment as shown in Fig. 4(a) when calculated using rotor geometry. The variation of revolution speed causes a periodic change in flow rate, pressure and torque. If it is assumed that the pressure difference between the upstream and the downstream of rotor is constant and there is no leakage through the rotor tip clearance, torque fluctuation can be calculated geometrically as shown in Fig. 4(b). For the torque calculation, the mean pressure between the upstream and the downstream of rotor is applied to that of the volumetric displacement, which is the enclosed region by the rotor circumferential wall and casing wall. As a result, it is recognized that the flow rate fluctuation becomes about ±10%, and in addition, torque acting on the rotor always acts to the direction of revolution (positive value). Torque fluctuation acting on an individual rotor becomes nearly ±50%, but the total sum of torque fluctuation becomes about ±10%.

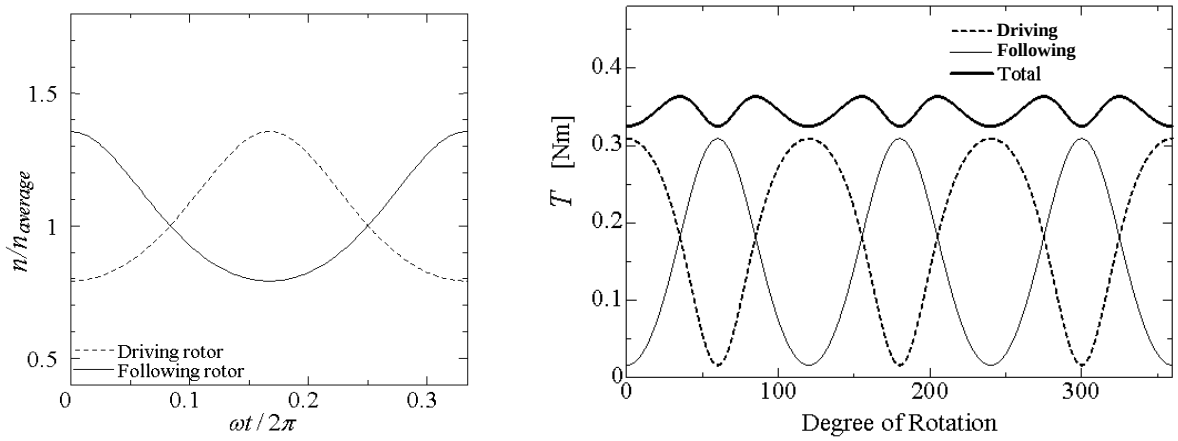

(a) Rotational speed of each axis (b) Torque variation

Fig. 4 Time dependent rotational speed and torque variations

3. Results and Discussions

3.1 Velocity Vectors and Pressure Pulsation

Calculated velocity vectors are illustrated in Fig. 5. Relatively uniform flow enters into the rotor inlet, which is located at left side of the rotor, but the flow at the rotor outlet forms strong vortices and a complicated flow pattern changes every moment with a rotation of the rotor. In the volumetric displacement is formed a large vortex that has the same rotational direction as the rotor, and strong leakage flows pass through the rotor tip clearances.

Figure 6 shows the comparison of pressure pulsation between the experiment and the calculation for the case of n=1000min^{-1}. As 6 times of discharge occur from the volumetric displacement when the 3-lobe rotor makes 1 rotation, the results during 1/3 rotation ($\omega t/2\pi$=1/3) is illustrated in Fig. 6. According to the results, the time averaged values and the pulsation amplitude of the calculated pressure correspond to about 80% and 50% of the measured values, respectively. To be remarked here is that two same pressure pulsation curves should be generated, when two 3-lobe rotors of the same configuration make 1/3 rotation, but that the measured pulsation curve shows a peculiar asymmetric curve. The calculated pressure obviously shows almost the same two pulsations, though the calculated result does not reproduce the experiment.

In this case, as the pressure difference Δp should receive considerable influence by the rotor configuration, such as tip clearance size and having gear or not, it is natural that the shape of pulsation curve by CFD has somewhat difference from that by experiment. However, because the shape of pulsation curve is based on the rotor rotation, it was expected that the shape of pulsation curve by CFD and experiment might agree well each other.

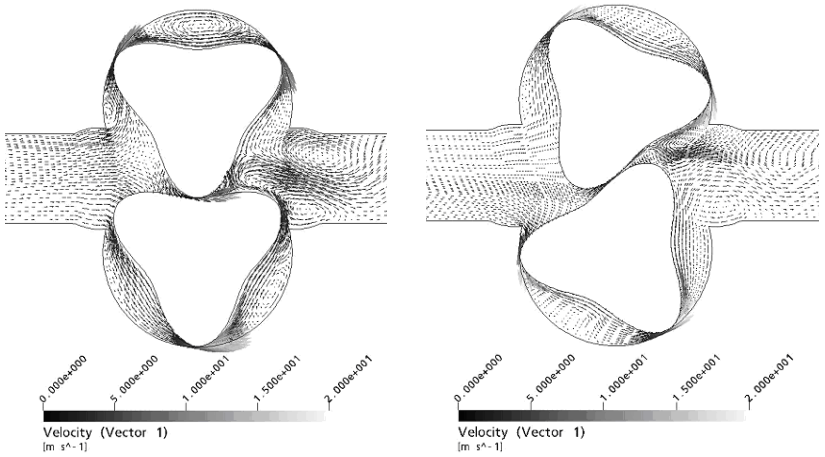

(a) $\omega t/2\pi = 0$ (b) $\omega t/2\pi = 0.05$

Fig. 5 Calculated velocity vector at two rotor positions

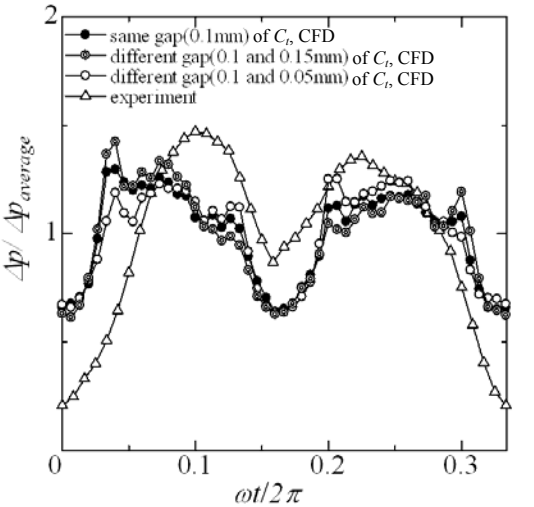

Fig. 6 Comparison of CFD with measurement of pressure pulsation

As it is considered that the reason of a peculiar shape is caused by the asymmetric shape of two rotors, that is, the difference of tip clearance C_t at each rotor, the calculated results for the different tip clearance C_t is also compared in Fig. 6. The calculated results reveal that, even if the tip clearance is remarkably different in two rotors, the shape of pulsation curve shows only a little difference each other and there exists still remarkable difference between the calculated and the measured pressure pulsation.

One another factor giving considerable influence on the pulsation curve is a rotational speed. Then, the rotational speed of the output axis is measured by experiment, and it is revealed that the driving rotor installed to output axis rotates at a constant speed as shown in Fig.7(a). In other words, when the load of a generator is applied to one axis, the loaded axis keeps constant rotational speed, but another free-load axis, the following axis, takes all the fluctuation of rotational speed. Accordingly, the change of

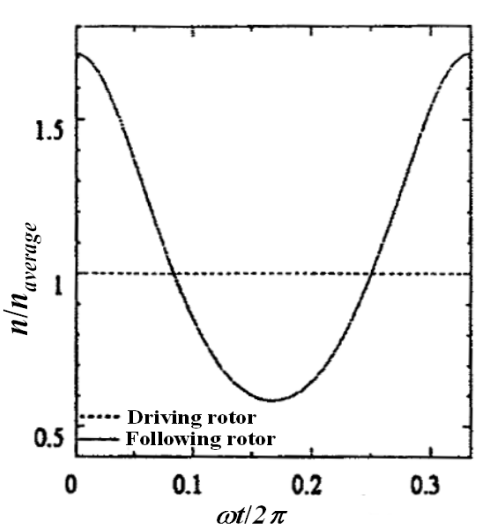

(a) Rotational speed fluctuation (experiment)

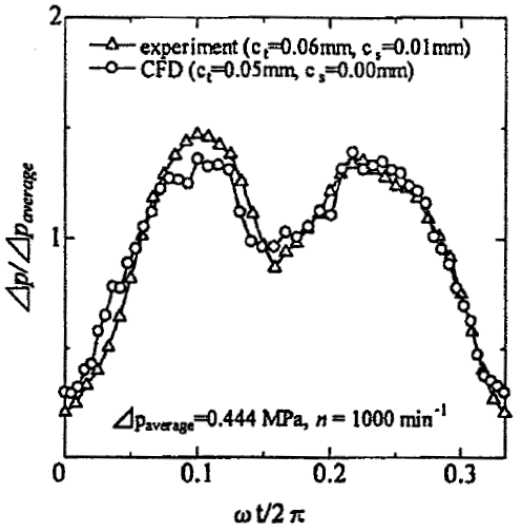

(b) Pressure pulsation

Fig. 7 Actual rotational speed and comparison of pressure pulsation

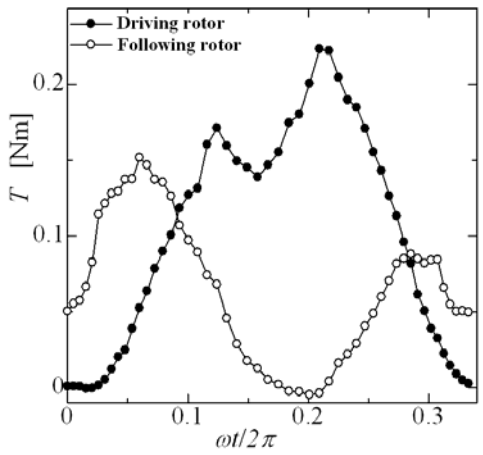

(a) Torque fluctuation acting on two rotors

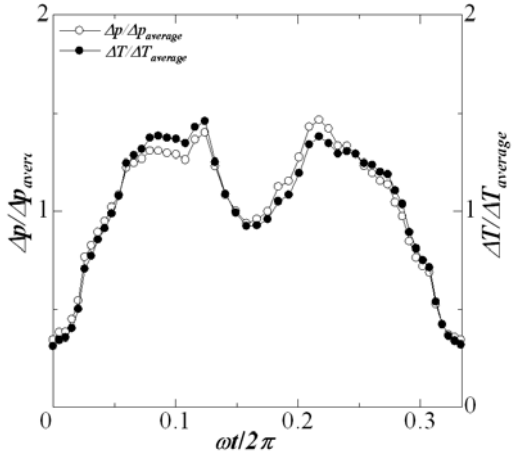

(b) Comparison of pressure and torque pulsation

Fig. 8 Comparison of torque variation (CFD)

rotational speed of the following rotor shows 0.6-1.7 times of the driving rotor. It is conjectured that the fluctuation is caused by the extremely small moment of inertia in the following rotor in comparison with that in the driving rotor. Figure 7(b) shows comparison of pressure pulsation curves between the experiment and the CFD, in which the result in Fig. 7(a) is used as an input rotational speed. The shapes of two pressure pulsation curves agree well each other.

After all, it is concluded that a large scale and peculiar shape of pressure pulsation curve occurring in the PDT are caused by a considerable fluctuation of rotational speed of the following rotor, and the constant rotational speed in the driving rotor is a very good operational condition as an output rotor of hydro turbine. In this case, the torque pulsations by driving rotor and following rotor show large difference as shown in Fig. 8(a), but the torque pulsation curve by the sum of two rotors becomes almost similar to the shape of the pressure pulsation curve as shown in Fig. 8(b).

In addition, in the case of a positive displacement pump, especially rotary pump, it is common to rotate the rotors with same rotational speed by connecting two rotors with a timing gear installed outside. However, if the rotational speed of two rotors in PDT is set to equal, there will be large leakage loss because it needs to make the center clearance C_c between two rotors to be large not to keep in contact with each other. Furthermore, for a micro hydro turbine used in such as a water faucet, the turbine size should be as smaller as possible and thus, the exterior timing gear system is not recommendatory for actual application.

When the differential pressure Δp in PDT pulsates as is in Fig. 7(b), pressure distribution along a rotor wall is shown in Fig. 9, where abscissa is the %-length along the rotor wall surface for one pitch (120deg.). The instantaneous pressure in an enclosed region of volumetric displacement becomes always equal to the mean value of the upstream and the downstream of rotor. Pressure undershoot shown in the figure is caused by a sudden pressure drop due to immediate acceleration of leakage through the rotor tip clearance. The reason why the pressure in the volumetric displacement is equal to the mean value is that the pressure in the volumetric displacement is regulated automatically so that two leakage flow rate through the tip clearances formed at the entrance and exit of the volumetric displacement becomes equal.

As this pressure distribution produces rotation torque to the rotor, the pressure undershoot produces torque loss. The theoretical torque is given by $T_{th}=\Delta p V_d$, and this is equivalent to the pressure distribution shown by the dotted line in Fig. 9. When calculating the torque loss from the pressure undershoot in Fig. 9, it amounts to 12% of total torque, and the calculated value agrees with the measured value of $C_{\Delta p}$=0.122 [6]. In other words, a pressure drop by the leakage occupies most of the torque loss in the PDT.

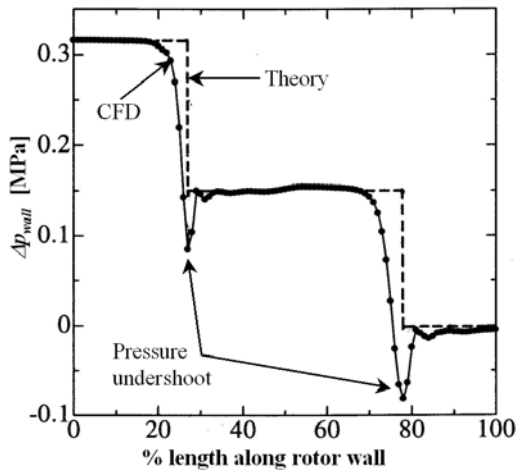

Fig. 9 Pressure distribution along rotor circumference

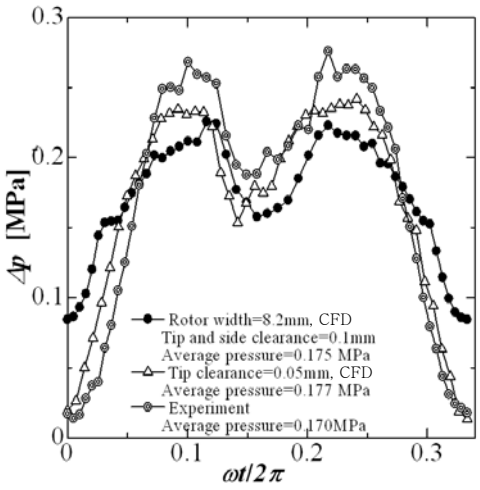

Fig. 10 Influence of side clearance on pressure pulsation

While, in order to examine the influence of side clearance, CFD analysis is carried out with the rotor height B=8.2mm, which is a half of the actual rotor, side clearance c_s=0.1mm and symmetric boundary condition on the other side clearance. Figure 10 compares the calculated differential pressure with the measured one in the cases of with side clearance (●) and without side clearance (Δ). According to the calculation results, if the calculation considers the side clearance, the time-averaged value of pressure pulsation does not change, but the pulsation amplitude reduces to a half. Even though the calculation considers a side clearance, the calculated result does not agree with the measured. The reason of disagreement is attributable to a large difference of side clearance between the actual case and the calculation, and the actual side clearance is c_s=0.01mm, 1/10 of the calculation. In such a narrow side clearance case, the present calculation has a limitation to calculate the flow field.

3.2 Mechanism of Pressure Pulsation and Its Characteristics

As the present unsteady calculation adopts an inlet condition of constant flow rate, a good agreement between the calculated and measured results means that there exists very small pulsation in flow rate. If there is no leakage in a positive displacement fluid machinery, flow rate is proportional to a rotational speed and thus, there should be considerable flow rate pulsation caused by a large rotational speed fluctuation. However, actually a large amount of leakage occurs through the tip and side clearances. Hence, the discharge to exit in PDT consists of two discharges, that is the discharge from the volumetric displacement and the leakage through the clearances, and the total sum of discharge is kept almost constant, which is the reason of considerably small flow rate pulsation, in spite of large rotational speed fluctuation.

Now we try to reveal the mechanism of large pressure pulsation. In case of positive displacement machinery, a fluid is confined in the region of volumetric displacement with a rotor rotation, in which the pressure becomes mean value of the upstream and downstream of a rotor. During this process, as there are always three or four points of very narrow tip clearance, very large fluid resistance, formed between the tips of one pair of rotor and casing wall, the differential pressure Δp between the upstream and downstream should take the maximum value for the case of four points of narrow tip clearance. However, according to Figs. 7 (a) and (b), regardless of the number of very narrow tip clearance, in other words, no relation with the magnitude of flow resistance, the differential pressure Δp takes the maximum when the absolute value of rotational speed fluctuation rate dn/dt becomes the maximum, and Δp takes the minimum at the time of dn/dt=0. The value of dn/dt corresponds to the acceleration of rotor revolution.

This result reveals that when the absolute value of dn/dt becomes larger, the delay in forming leakage becomes longer and then, Δp becomes increased so as to keep constant total flow rate. Moreover, when dn/dt is small, leakage follows immediately and then, Δp becomes small. On the other hand, as the power of the upstream fluid is almost constant, the torque T and differential pressure Δp becomes the minimum when rotational speed n takes the maximum. Consequently, this might be the mechanism of large pressure pulsation in the positive displacement fluid machinery.

In order to clarify the pressure pulsation characteristics, measured and calculated pulsation amplitudes are summarized for the changes of rotational speed and differential pressure as shown in Fig. 11. It is revealed from the results that the pressure pulsation amplitude increases in proportion to 3/5th power of rotational speed n and to 2/3rd power of differential pressure Δp.

3.3 Steady Performances

The pressure pulsation characteristics can be clarified only by an unsteady calculation, but the steady performance can be analyzed by a quasi-steady calculation. Figure 12 shows the comparison of calculated results by both the unsteady and quasi-steady calculations for the tip clearance leakage characteristics, which have largest influence on the steady performances of a turbine. Side clearance is not considered for the calculations.

In the quasi-steady calculation the flow at the time of the specific rotor position is calculated and only the leakage flow rate Q_l through the rotor tip clearance can be obtained. Thus, the total flow rate Q is treated as the sum of calculated Q_l and theoretical flow rate $Q_{th}=V_d n$ /60. From Fig.12(a) leakages obtained by the quasi-steady and unsteady calculations agree well each other, and from Fig.12(b) the output torque T obtained by quasi-steady calculation agrees well with the measured value.

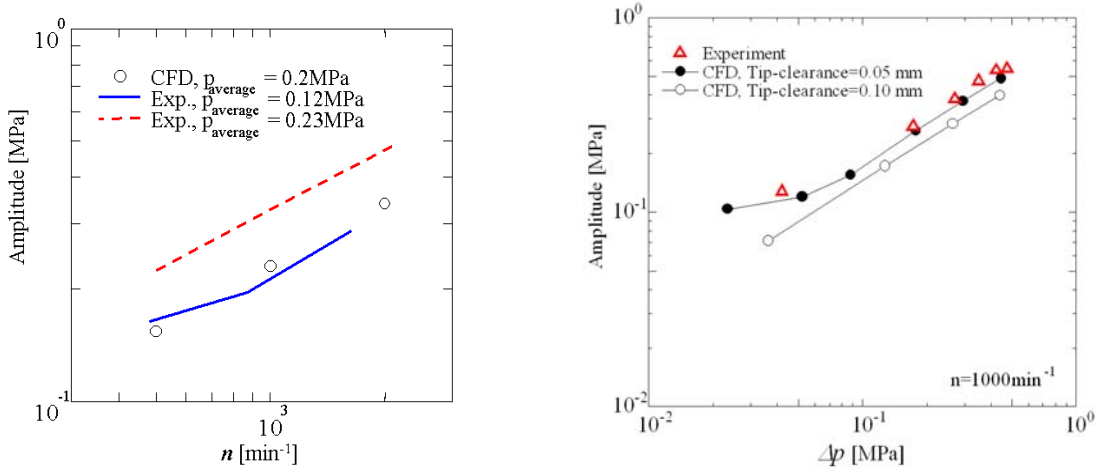

(a) Rotational speed change (b) Differential pressure change

Fig. 11 Change of amplitude of pressure pulsation vs. rotational speed and pressure level

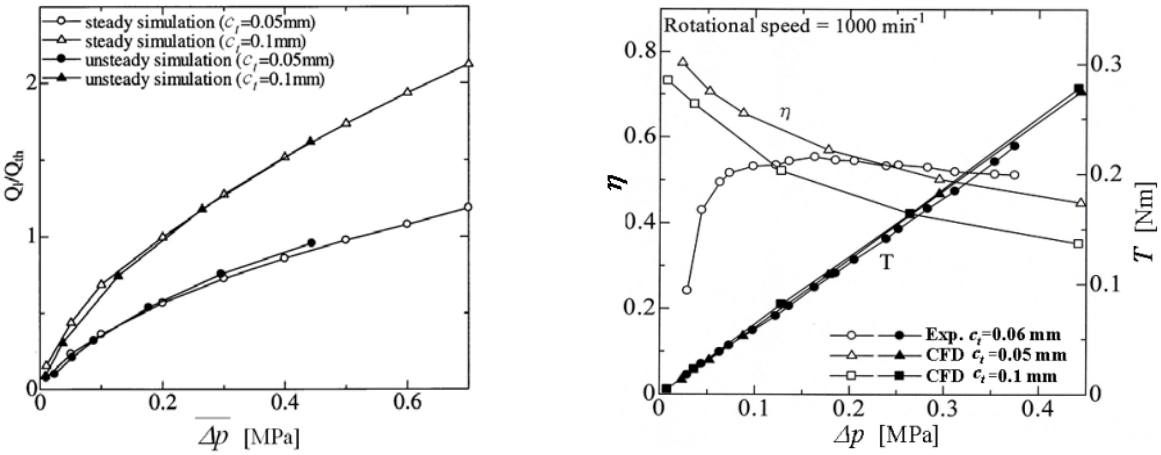

(a) Leakage characteristics (CFD) (b) Torque characteristics

Fig. 12 Comparison of unsteady and steady CFD simulations

However, as for efficiency, the measured results become closer to 0 in the small $\overline{\Delta p}$ range because of small loss torque by mechanical friction at seal and bearing, but the calculated results become closer to 1.0 in the range of small $\overline{\Delta p}$ because the mechanical friction is not considered in the calculation at all. In the relatively large $\overline{\Delta p}$ range, the efficiencies by measurement and calculation agree well because the output torque T becomes significantly large compared with loss torque.

As the actual test rotor has 33 pieces of small gear around the rotor, verification of its influence on the turbine performances is necessary. Thus quasi-steady calculation is performed at the tip clearance of c_t=0.1mm and no side clearance, and the calculated velocity vectors are shown in Fig. 13. Comparing the flow patterns of gearless case (Fig. 13(a)) with geared case (Fig. 13(b)), it is clearly shown that the flows in the tip clearance and exit in the geared case shows stronger jet through the tip clearance and larger

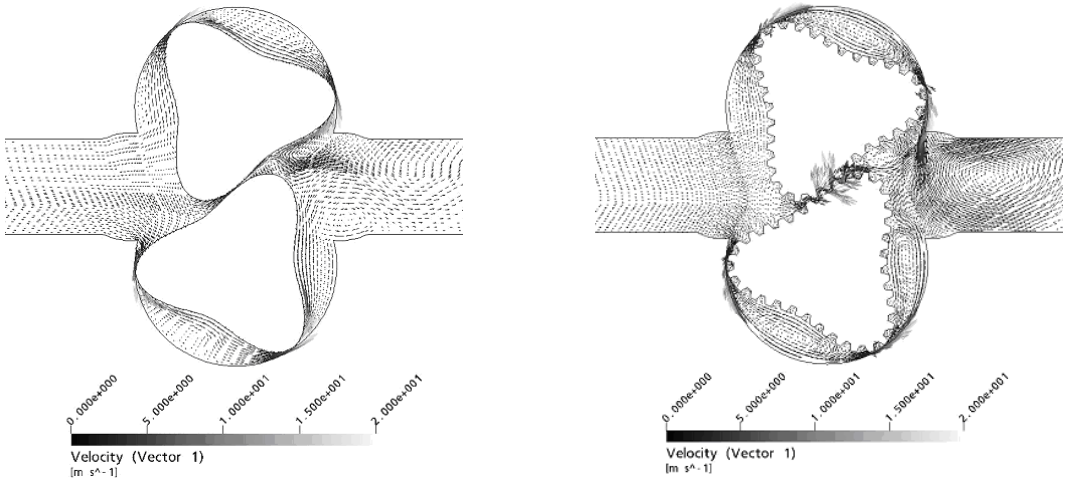

(a) Gearless case (b) Geared case

Fig. 13 Comparison of velocity vectors between the geared and gearless cases (CFD)

vortex at the exit than the gearless case. As for the leakage flow through tip clearance, the flow resistance in the geared case becomes twice of the gearless case, because the geared rotor has 2 pieces of gear at a narrow tip clearance. Therefore, leakage through tip clearance of the geared case can be roughly estimated to $1/\sqrt{2} = 0.71$ times of the gearless case. The calculated result supports the above estimation of leakage, that is 0.70 times of the leakage.

3.4 Proposal of Low Pulsation PDT

From the above discussions it has been revealed that pressure pulsation increases remarkably with an increase of rotational speed and differential pressure in a 3-lobe straight type PDT. According to the study by Phommachanh et al. [6], only a half of the pressure pulsation at the rotor upstream can be reduced by using a surge tank. Thus, the pressure pulsation is the most difficulty in applying the present turbine for practical use. As it is revealed that the pressure pulsation is caused by the formation delay of the leakage through the rotor tip clearance, namely, is closely related to the instantaneous shutoff of the volumetric displacement, there needs improvement of the shutoff time of the rotor for further reduction of pulsation.

As a trial of delaying the shutoff time, it is considered effective to move the rotor tip contact point to the axial direction. Here is proposed a helical lobe type rotor, which is twisted in the axial direction. Lobe number and twisted angle of the adopted rotor for experiment are 4 pieces and γ = 11deg., respectively.

The comparison of pressure pulsations between the straight 3-lobe type rotor and the helical 4-lobe type rotor is shown in Fig. 14(a) under the same time-averaged differential pressure. The pressure pulsation in the helical 4-lobe type is compared under various pressure levels in Fig. 14(b). It is clearly seen from Fig. 14(a) that the pulsation amplitude by helical 4-lobe type rotor is considerably reduced to about 20% of that by straight 3-lobe type rotor. In this case, the pulsation amplitude at the rotor exit changes little, as the downstream pipe exit is open to the atmosphere. According to Fig. 14(b), if the differential pressure is increased by 4 times, then the pulsation amplitude increases by 3 times, and if the rotational speed is increased by 4 times, the pulsation amplitude increases by 2times, though not shown in the figure. After all, the helical lobe type generates considerably low pulsation compared with that of straight lobe type, and the pulsation is insignificant level.

As the contact point of two lobes at the center clearance changes every moment in the helical lobe type, there is a possibility of efficiency drop due to the increase of leakage. The measured torque and efficiency performances are thus shown in Fig. 15. As the size of helical lobe type used in this study is much larger than the straight lobe type, and the flow rate per revolution of helical

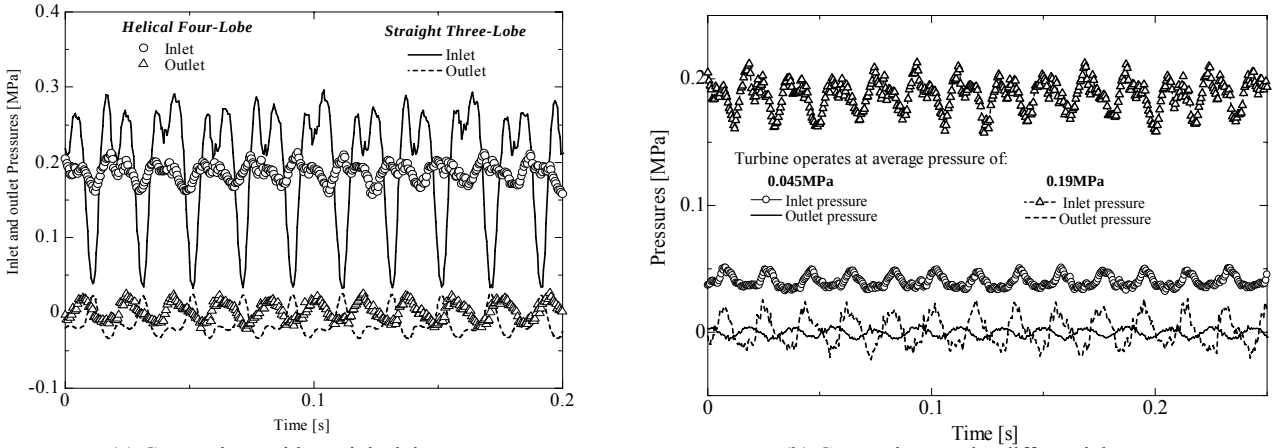

(a) Comparison with straight-lobe type (b) Comparison under differential pressure

Fig. 14 Pressure pulsation caused by helical 4-lobe rotor (experiment)

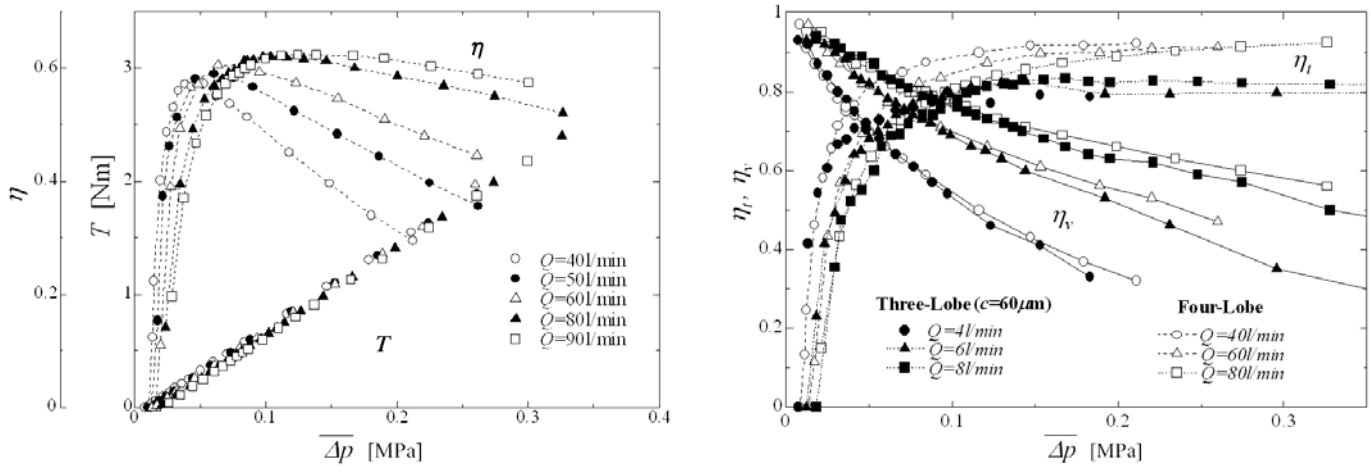

(a) Efficiency and torque vs. pressure difference (b) Torque efficiency and volumetric efficiency

Fig. 15 Performances of helical 4-lobe turbine (experiment)

lobe type is about 10 times that of straight lobe type, 10 times of flow rate is used for the experiment. Figure 15 reveals that torque and leakage in the helical 4-lobe type turbine are almost dependent only on the differential pressure same as the straight 3-lobe type [6], but torque efficiency becomes much higher. This is because the fluid shutoff becomes gentle and thus, the torque loss by pressure undershoot is considerably reduced. In addition, both the torque efficiency η_t and the volumetric efficiency η_v of the helical lobe type become larger in the higher flow rate range than those of straight lobe type, and as a result, high efficiency range becomes wider in the case of larger flow rate as shown in Fig. 15(a).

According to the present study, empirical equations can be derived in a general form for flow rate Q, volumetric efficiency η_v and torque efficiency η_t through the experimental analysis method [6], The equations are expressed as follows;

$$\text{Flow rate}: \quad Q = Q_{th} + Q_l = nV_d/60 + 0.380A(2\overline{\Delta p}/\rho)^{0.58} \quad (\text{m}^3/\text{s}) \tag{1}$$

$$\text{Volumetric efficiency}: \quad \eta_v = Q_{th}/(Q_{th} + Q_l) = 1/(1 + 0.620A\overline{\Delta p}^{0.58}/V_d n) \tag{2}$$

$$\text{Torque efficiency}: \quad \eta_t = (T_{th} - T_l)/T_{th} = 0.917 - 9.81n/\overline{\Delta p} \tag{3}$$

Total efficiency can be calculated by $\eta = \eta_t \times \eta_v$. If the specifications are given, the optimum dimensions can be determined using above equations [6].

4. Conclusions

Unsteady flow in a straight 3-lobe rotor type PDT is analyzed and pressure pulsation characteristics are clarified by CFD and experiment. Moreover, low pulsation type helical 4-lobe rotor is proposed and its steady performance is determined experimentally. The conclusions are summarized as follows.

1. A large and peculiar pressure pulsation in a straight lobe type PDT is caused both by fluid shutoff of volumetric displacement and by a large rotational speed fluctuation of the following rotor. Rotational speed in a driving rotor is kept constant, which can be a good advantage for practical application of the present turbine.
2. Pressure pulsation amplitude can be estimated by unsteady calculation, and the pulsation amplitude increases in proportion to 3/5th power of rotational speed and 2/3th power of differential pressure. Moreover, steady performance of the turbine can be well estimated by quasi-steady calculation.
3. It is conjectured that a large pressure pulsation in the straight lobe type PDT is mainly caused by the time delay in forming leakage through a rotor tip clearance.
4. The pressure pulsation amplitude in the straight type rotor can be reduced to about one fifth and insignificant level using a helical type rotor.
5. Helical rotor is effective for the improvements of torque efficiency and total efficiency in comparison with the geared type straight rotor.
6. Pressure in the enclosed region of volumetric displacement is always equal to the mean pressure of the upstream and downstream, and pressure undershoot caused by flow acceleration in a rotor tip clearance occupies large proportion of torque loss.
7. The pressure pulsation causes a torque pulsation, and both of the pulsation curves almost agree with each other.

According to the result of present study, it has been clarified that low pulsation type positive displacement hydro turbine proposed here is suitable for the micro hydropower generation in the very low specific speed range, which is lower than that of impulse type hydro turbine. If this turbine is applied to various types of large capacity valve, a large amount of wasted micro hydro resources can be recovered effectively.

Acknowledgments

The authors express their appreciation to Mr. N. Ichijo and Dr. D. Phommachanh of Yokohama National University for their enthusiastic efforts on the CFD analysis and experiment. Also, the authors wish to express their thanks to Mr. T. Motohashi and Dr. K. Matsumoto of TATSUNO Mechatronics Co. Ltd, Japan for their many useful advices and Mr. N. Nakajima of URO Co. Ltd. for his cooperation on an experimental setup.

Nomenclature

A	Total area of tip clearance [m^2]	Q_{th}	Theoretical flow rate [m^3/s]
B	Height of rotor [mm]	T	Torque [Nm]
$C_{\Delta p}$	Coefficient of differential pressure loss torque	T_l	Loss torque [Nm]
c_c	Center clearance [μm]	T_{th}	Theoretical torque
c_s	Side clearance [μm]	t	Time [sec.]
c_t	Tip clearance [μm]	V_d	Volumetric displacement of rotor
D	Diameter of test rotor	γ	Twisted lobe angle
H	Effective head [m]	η	Total efficiency

n	Rotational speed [min^{-1}]	η_t	Torque efficiency
Δp	Differential pressure between entrance and exit [Pa]	η_v	Volumetric efficiency
$\overline{\Delta p}$	Time mean differential pressure [Pa]	ρ	Fluid density [kg/m^3]
Q	Flow rate [m^3/s]	ω	Angular speed [rad/s]
Q_l	Leakage flow rate [m^3/s]		

References

[1] Harvey, A., Brown, A., Hettiarachi, P. and Inversin, A., 2005, Micro-Hydro Design manual – A guide to Small-Scale Water Power Schemes, ITDG Publishing, UK.

[2] Davis, S., 2003, Microhydro : Clean Power from Water, New Society Publisher, Canada.

[3] Thake, J., 2000, The Micro-Hydro Pelton Turbine Manual, ITDG Publishing, UK.

[4] Khennas, S. and Barnett, A., 2000, "Best Practices for Sustainable Development of Micro hydro Power in Developing countries," Report for The Department for International Development, UK and The World Bank (Contract R7215), The Schumacher Centre for Technology and Development, UK.

[5] Dhanapala, K. and Wijayatunga, P., 2002, "Economic and Environmental Impact of Micro-Hydro- and Biomass-Based Electricity Generation in the Sri Lanka Tea Plantation Sector," Energy for Sustainable Development, Vol. VI, No. 1, pp. 47-55.

[6] Phommachanh, D., Kurokawa, J., Choi, Y-D. and Nakajima, N., 2006, "Development of a Positive Displacement Micro-Hydro Turbine," *JSME Internatinal Journal*, Series B, Vol. 49, No. 2, pp.482-489.

[7] The Japan Fluid Power System Society, 2003, Hydraulic Pressure Drive Text Book (in Japanese).

[8] ANSYS Inc., 2004, ANSYS CFX Documentation Ver.5.7.1.